Role of oxygen in superconductivity of $Nd_{2-x}Ce_xCuO_{4-y}$ studied by x-ray-absorption near-edge structure

Hiroyuki Oyanagi, Yuko Yokoyama, and Hirotaka Yamaguchi
Electrotechnical Laboratory, Umezono, Tsukuba, Ibaraki 305, Japan

Yuji Kuwahara
The Institute of Physical and Chemical Research, Wako-shi, Japan

Toshikazu Katayama and Yoshikazu Nishihara
Electrotechnical Laboratory, Umezono, Tsukuba, Ibaraki 305, Japan
(Received 12 July 1990)

The effect of reduction on the electron states of $Nd_{2-x}Ce_xCuO_{4-y}$ ($0.15<x<0.17$) has been revealed by x-ray-absorption near-edge structure on the Cu K edge for a series of samples annealed at various oxygen partial pressures ($pO_2=1-10^{-3}$ atm). We find that the Ce doping-induced states in the near-edge structure systematically increase the magnitude with the decrease of oxygen partial pressure, well correlating with the oxygen pressure dependence of superconducting fraction and T_c value. The results indicate that the reduction strongly enhances the electron density at the copper sites, through the removal of a small number of defect oxygen atoms that suppress n-type doping in the CuO_2 plane.

I. INTRODUCTION

$Nd_{2-x}Ce_xCuO_{4-y}$ contrasts previously known high-T_c superconductive cuprate compounds in that the major charge carriers are electrons rather than holes.[1] In this system, as-prepared samples are not superconductive upon Ce doping. Superconductivity is observed over the narrow Ce concentration range ($0.14<x<0.18$), only after heat treatment under reducing conditions.[1,2] Although the nature of charge carriers has been extensively studied,[3-10] there still remain several important problems which have not been resolved yet, such as the location of charge carriers and the role of oxygen in superconductivity. As for the location of doped carriers, contradicting experimental results or even different interpretations of the same results have been reported. Initial x-ray-absorption near-edge studies[3,5] reported the formation of Cu^+ (d^{10} configuration) upon Ce doping, indicating that doped electrons occupy the Cu $d_{x^2-y^2}$ states. On the other hand, photoemission study[7] and more recent x-ray absorption studies suggested that doped electrons occupy other states, such as the Cu 4s states,[4] or they form the impurity states near the Fermi level,[6] while later photoemission studies supported the formation of Cu^+ as a result of Ce doping.[8-10]

The role of reduction in superconductivity is an interesting, yet another puzzling problem since the additional carrier concentration due to the oxygen nonstoichiometry change during reduction[11-16] is much smaller than that originating from Ce^{4+} doping. Such a small change of oxygen deficiency cannot account for a large change in the apparent carrier density as observed in the Hall coefficient experiment.[17] Moreover, the presence of excess oxygen atoms[14,16] now provides a possibility of hole doping or additional electron doping, depending on whether the mobile oxygen atoms are incorporated or removed. In order to investigate the role of oxygen in superconductivity, we have performed a systematic x-ray-absorption near-edge structure measurement on $Nd_{2-x}Ce_xCuO_{4-y}$ ($0.15<x<0.17$) prepared at various oxygen partial pressures. The effect of oxygen partial pressure p_{O_2} during heat treatment on the Cu K near-edge structure which provides direct information on the doping-induced states at the copper sites is carefully analyzed. The result shows that annealing at low p_{O_2} increases the magnitude of Ce doping-induced states in the near-edge structure, which correlates well with the superconducting fraction and T_c value. The active role of reduction in the enhancement of carrier density in the CuO_2 plane has been confirmed.

II. EXPERIMENT

$Nd_{2-x}Ce_xCuO_{4-y}$ samples were synthesized from a mixture of CuO_2, Nd_2O_3, and CuO as reported in Ref. 1. The mixed powder was calcined in air at 950 °C for 10 h and pressed into pellets. The pellets were sintered at 1100 °C for 10 h and slowly air cooled to room temperature. A series of samples to study the effect of reduction were prepared by annealing the sintered pellets at 1050 °C for 20 h with various oxygen partial pressures ($p_{O_2}=1-10^{-4}$ atm) in an argon-oxygen gas mixture. Some of the pellets were also annealed at 900 °C and quenched to room temperature in a pure argon atmosphere. The oxygen deficiency y was monitored by an inert gas fusion nondispersive ir method. Powder x-ray diffraction measurements confirmed that all samples are

single-phase materials. X-ray absorption experiments were performed using synchrotron radiation from the 2.5-GeV storage ring at the Photon Factory. The Cu K-edge spectra were obtained in a transmission mode. The energy resolution is approximately 2 eV at 9 keV using an encoded Si(111) double-crystal monochromator. The energy scale was calibrated by recording the Cu metal data with the characteristic feature indicating the Fermi level (8980.3 eV). All spectra were sequentially measured at room temperature to minimize the experimental error in an energy scale. The experimental error in energy is within 0.1 eV.

The polarized near-edge spectra were measured for single-crystal Pr_2CuO_4 grown by a flux method. The angle between the electrical field vector and the c axis θ, was chosen to obtain the in-plane ($\theta=90°$) and out-of-plane ($\theta=10°$) polarized spectra. The Cu $K\alpha$ fluorescence yield spectra were recorded using an array of nine NaI scintillation detectors. A fluorescence detection mode was shown to be equivalent to a transmission mode because of strong absorption of emitted fluorescence x-rays by heavy elements in cuprate compounds such as La_2CuO_4,[18] i.e., Pr atoms in the case of Pr_2CuO_4.

III. RESULTS AND DISCUSSION

In Fig. 1 polarized Cu K-edge spectra for single-crystal Pr_2CuO_4 are shown in the upper column together with the powder data for $Nd_{1.85}Ce_{0.15}CuO_{4-y}$ and Nd_2CuO_4 in the lower column. The near-edge features observed at 8980–9006 eV are strongly polarized with respect to the orientation of the basal plane. The fine structures c and d in the in-plane ($\theta=90°$) polarized data are assigned to the $1s$-$4p^*(\sigma)$ quasibound-state transitions, whereas the pre-edge features a and b observed in the out-of-plane ($\theta=10°$) data are due to the $1s$-$4p^*(\pi)$ transitions. The lower-energy features a and c arise from the final-state effect with the presence of ligand-to-metal charge transfer.[19] The satellite-to-main peak intensity ratio (I_a/I_b) for the $1s$-$4p^*(\pi)$ transition is larger in the T' phase than in the T phase.[18] This indicates that the d^{10} contribution in the ground state is larger in the former since the satellite peak originates from the final state $3d^{10}\underline{L}$, where $\underline{L}$ denotes a hole in the ligand orbital.[19] Both satellite and main peaks of the $1s$-$4p^*(\pi)$ transition are broad and thus partly overlap with the $1s$-$4p^*(\sigma)$ transitions or the onset of continuum, suggesting an extended nature of the $4p^*(\pi)$ states in the T' phase. The observed near-edge structures for powder Nd_2CuO_4 can be assigned to features a–d in the polarized data of Pr_2CuO_4; shoulderlike features observed at 8983 and 8992 eV in the powder spectrum are attributed to a and b, respectively, while the twin peaks observed around the absorption maximum are due to features c and d. As reported previously,[3–6] the effect of Ce doping is most significantly observed around features a–d; the pre-edge region around features a and b increases the intensity, while features c and d decrease the intensity upon Ce doping.

Figure 2 shows the Cu K near-edge spectra for $Nd_{1.85}Ce_{0.15}CuO_{4-y}$ annealed at various p_{O_2} ($1-10^{-3}$ atm) plotted on an expanded energy scale. In the lower column, the near-edge spectrum for Nd_2CuO_4 is superimposed on the data for $Nd_{1.85}Ce_{0.15}CuO_{4-y}$ annealed in a pure argon atmosphere under the strongest reducing condition. Features A–E indicate the positions of characteristic features in difference spectra which increase in magnitude with the increase of x.[3–6] The near-edge structure gradually changes as a function of p_{O_2} in a similar manner with the change associated with Ce doping; i.e., the shoulderlike features a and b increase the intensity, while features c and d decrease the intensity as p_{O_2} is lowered.

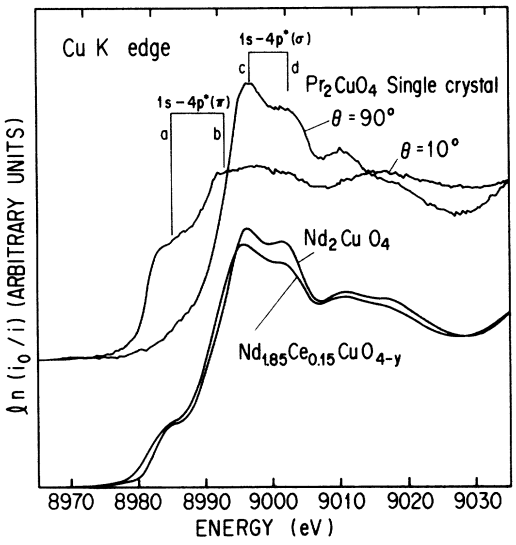

FIG. 1. Polarized Cu K-edge spectra for single-crystal Pr_2CuO_4 (upper curves) together with powder data for pure Nd_2CuO_4 and reduced $Nd_{1.85}Ce_{0.15}CuO_{4-y}$ (lower curves). θ denotes an angle between the electrical-field vector E and the c axis.

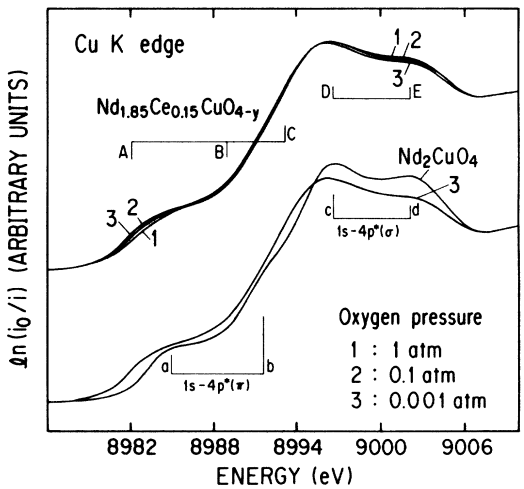

FIG. 2. Cu K near-edge spectra for $Nd_{1.85}Ce_{0.15}CuO_{4-y}$ reduced by annealing at oxygen pressures $p_{O_2}=1$, 10^{-1} and 10^{-3} atm at 1050 °C (upper curves). The data for $Nd_{1.85}Ce_{0.15}CuO_{4-y}$ annealed in pure argon atmosphere are compared with that of Nd_2CuO_4 (lower curves).

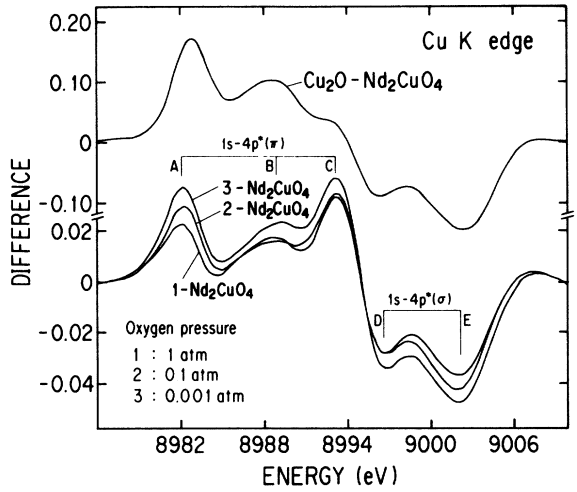

FIG. 3. Cu *K*-edge difference spectra for $Nd_{1.85}Ce_{0.15}CuO_{4-y}$ ($p_{O_2}=1$, 10^{-1}, and 10^{-3} atm) obtained by subtracting the absorption spectrum for pure Nd_2CuO_4 from the data shown in Fig. 4 (lower curves). The data for Cu_2O are also shown scaled down by a factor of 0.5 (upper curve).

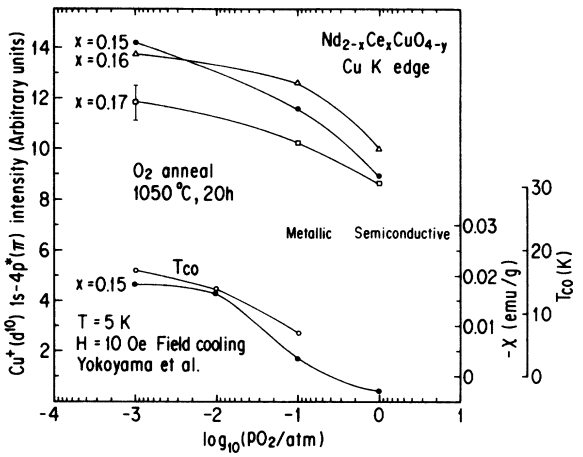

FIG. 4. Intensity of the Ce doping-induced states (8982 eV) for $Nd_{2-x}Ce_xCuO_{4-y}$ with $x=0.15$–0.17 annealed at $p_{O_2}=1$, 10^{-1}, and 10^{-3} atm. The diamagnetic fraction with a field of 10 Oe at 5 K and onset T_c value determined from resistivity are also shown in the lower column. The shaded region indicates the boundary between semiconductive and metallic regions beyond which superconductivity apparently initiates.

In Fig. 3 the difference spectra between the raw data for $Nd_{1.85}Ce_{0.15}CuO_{4-y}$ and the standard Nd_2CuO_4 data are shown where each spectrum was normalized at isobetic points (8973 and 9029 eV) before subtracting the standard data. The energy positions of characteristic features in the difference and raw spectra are listed in Table I. With the decrease of p_{O_2}, features A–E gradually increase the intensity in a similar manner with the previously reported Ce concentration dependence.[3–6] The presence of Cu^+ was first indicated based on the fact that features A, B, D, and E are also observed in the difference spectrum for Cu_2O,[3,5] while the absence of feature C led to the different conclusion that doped electrons occupy other states.[4] It might be worthwhile to note that, in case of $Ba_2YCu_3O_y$ ($6<y<7$), similar characteristic features are observed in difference spectra as the Cu^+ is formed in the Cu1 sites with the decrease of y.[20] Also in difference spectra for oxygen-deficient $Ba_2YCu_3O_y$, the shoulder region corresponding to features B and C in Cu_2O data are not reproduced, suggesting that this region is sensitive to the coordination geometry, in particular, projected along the c axis and may not be directly compared. However, since the magnitude of feature A correlates well with the carrier density measured by the Hall effect,[17] we believe that feature A reflects the carrier density at the copper sites, possibly, electrons occupying the Cu d-holes.

Figure 4 shows that the magnitude of feature A increases as a function of p_{O_2} for samples with $x=0.15$–17. Numerical values are summarized in Table II. The observed enhancement by heat treatment is most significant for a sample with $x=0.15$, which exhibits the highest T_c value (23 K).[1,2] The intensity increased by as much as 60% as p_{O_2} is lowered from 1 to 10^{-3} atm. This behavior correlates well with the diamagnetic fraction χ measured in a magnetic field of 10 Oe at 5 K.[21] In Fig. 4 the onset T_{c0} values determined from the temperature dependence of resistivity[21] are also shown. The temperature dependence of resistivity is semiconductive for samples with $p_{O_2}=1$ atm, while samples with $p_{O_2}<10^{-1}$ atm exhibit metallic temperature dependence of their resistivity. Superconductivity is observed above the crossover between the semiconductive and metallic regions[1,2] indicated by a shaded boundary in Fig. 4. From this figure it is natural to expect that the oxygen vacancies are somehow introduced during heat treatment, although oxygen nonstoichiometry change is negligible.

It has been recently recognized that the initially reported oxygen nonstoichiometry 0.04 determined by a titration method[1] is severely overestimated due to the reduction of Ce^{4+} and the presence of Cu^+. The oxygen deficiency y in $Nd_{1.85}Ce_{0.15}CuO_{4-y}$ is less than 0.008 ac-

TABLE I. Energy positions of characteristic features in the near-edge spectra.

Feature	*A*	*B*	*C*	*D*	*E*
energy (eV)	8982.9	8989.1	8993.0	8996.6	9002.3
	a	*b*		*c*	*d*
	8985.1	8991.6		8996.6	9002.3

TABLE II. Normalized intensity of the characteristic feature A for $Nd_{2-x}Ce_xCuO_{4-y}$ as a function of oxygen partial pressure. Intensity is normalized to the Cu_2O data. $\Delta I_A=[I_A(10^{-3})-I_A(1)]/I_A(1)$. Values in parenthesis indicate uncertainty in the last digit.

	Normalized intensity I_A p_{O_2} (atm)			
Specimen	1	10^{-1}	10^{-3}	ΔI_A
$Nd_{2-x}Ce_xCuO_{4-y}$				
$x=0.15$	0.137(8)	0.179(8)	0.219(8)	0.60
$x=0.16$	0.154(8)	0.194(8)	0.209(8)	0.36
$x=0.17$	0.133(8)	0.157(8)	0.182(8)	0.37
Cu_2O	1.0			

cording to a recent thermogravimetric study.[15] In the present study, no systematic change in y was observed as p_{O_2} was varied within experimental error. Let us assume that the reduction-induced oxygen vacancies increase the carrier density by $2(y'-y)$, where y and y' denote the oxygen deficiency before and after heat treatment, respectively. If we assume charge neutrality, the relative change in the intensity of feature A is given by $\Delta I_A=2(y'-y)/(x+2y)$, where ΔI_A is listed in Table II. Since $\Delta I_A=0.6$ for a sample with $x=0.15$, and if the upper limit of oxygen nonstoichiometry after reduction[15] $y'=0.01$ is used, we obtain an unrealistic negative y value. Thus the oxygen deficiency is much smaller than the change in carrier density, and a simple scheme of electron doping by oxygen vacancies is inadequate.

There has been no structural evidence for oxygen vacancies introduced during the reducing process; the results of the structural refinement of powder neutron-diffraction data were essentially the same for samples with and without reduction,[12,13] suggesting that oxygen vacancies introduced by reduction are not located at normal oxygen sites in the T' structure considered in the refinement process. However, the presence of excess oxygen atoms in Ce-doped Nd_2CuO_4 were recently reported,[14,16] which can be reversibly added or removed by oxygen or vacuum annealing. Such excess oxygen atoms may be located on the apical oxygen sites, which are normally empty in the ideal T' structure, or as defects in the interstitial site $(\frac{1}{4},\frac{1}{4},\frac{1}{4})$ in the unit cell of the tetragonal T structure as in the case of oxygen-rich La_2CuO_{4+y}.[22]

The presence of apical oxygen atoms is unfavorable for doping electrons due to the repulsive Coulomb interaction as shown by the calculation of Madelung energy by Kondo and Nagai.[23] Therefore, it is reasoned that a small amount of excess oxygen atoms at the apical sites which have prevented doped electrons from "residing" in the CuO_2 plane is removed by heat treatment. Doped electrons are provided into the conductive plane if the apical oxygen atoms are removed, thereby increasing superconducting fraction. If such weakly bound oxygens are trapped in the interstitial defect sites, there would be no large change in the total oxygen stoichiometry as observed. Indeed, Sr doping removes apical oxygen atoms and forms interstitial oxygen defects in $La_{2-x}Sr_xCuO_4$.[24] The fact that excess oxygen atoms decrease in number with the increase of x (Ref. 16) may also explain why the Hall coefficient R_H rapidly decreases its magnitude with the increase of x above the critical value for superconductivity.[2]

IV. CONCLUSION

The effect of annealing under reducing conditions on electron states at the copper sites in $Nd_{2-x}Ce_xCuO_{4-y}$ $(0.15<x<0.17)$ has been studied by the Cu K near-edge structure for samples annealed at various p_{O_2} $(1-10^{-3}$ atm). The Ce doping-induced characteristic near-edge features systematically increase their intensity with the decrease of p_{O_2}, which correlates with the superconducting fraction and T_c value. These results indicate that the carrier density in the CuO_2 plane is strongly enhanced by the rearrangement of oxygen atoms during reduction. A large increase in carrier density despite a small change in oxygen nonstoichiometry after reduction may occur if the excess oxygen atoms at the apical sites which suppress electron doping in the CuO_2 plane are removed.

ACKNOWLEDGMENTS

The authors appreciate invaluable discussions with J. Kondo and K. Kajimura. The Pr_2CuO_4 single crystal was kindly provided by H. Unoki and K. Oka. This work has been performed as a part of a project (Proposal No. 87-065) approved by the Photon Factory Program Advisory Committee.

[1]Y. Tokura, H. Takagi, and S. Uchida, Nature **337**, 345 (1989).
[2]H. Takagi, S. Uchida, and Y. Tokura, Phys. Rev. Lett. **62**, 1197 (1989).
[3]J. M. Tranquada, S. M. Heald, A. R. Modenbaugh, G. Liang, and M. Croft, Nature **337**, 720 (1989).
[4]E. E. Alp, S. M. Mini, M. Ramanathan, B. Dabrowski, D. R. Richards, and D. G. Hinks, Phys. Rev. B **40**, 2617 (1989).
[5]G. Liang, J. Chen, M. Croft, K. V. Ramanujachary, and M. Greenblatt, Phys. Rev. B **40**, 2646 (1989).
[6]N. Kosugi, Y. Tokura, H. Takagi, and S. Uchida, Phys. Rev. B **41**, 131 (1989).
[7]A. Fujimori, A. Tokura, H. Eisaki, H. Takagi, S. Uchida, and E. Takayama-Muromachi (unpublished).
[8]S. Uji, M. Shimoda, and H. Aoki, Jpn. J. Appl. Phys. **28**, L804

(1989).
[9]H. Ishii, T. Koshizawa, H. Kataura, T. Hanyu, H. Takai, K. Mizoguchi, K. Kume, I. Shiozaki, and S. Yamaguchi, Jpn. J. Appl. Phys. **28**, L1952 (1989).
[10]Y. Fukuda, T. Suzuki, M. Nagoshi, Y. Syono, K. Oh-ishi, and M. Tachiki, Solid State Commun. **72**, 1183 (1989).
[11]E. Takayama-Muromachi, F. Izumi, Y. Uchida, K. Kato, and H. Asano, Physica C **159**, 634 (1989).
[12]F. Izumi, Y. Matsui, H. Takagi, S. Uchida, Y. Tokura, and H. Asano, Physica C **158**, 433 (1989).
[13]G. H. Kwei, S.-W. Cheong, Z. Fisk, F. H. Garzon, J. A. Goldstone, and J. D. Thompson, Phys. Rev. B **40**, 9370 (1989).
[14]E. Moran, A. I. Nazzal, T. C. Huang, and J. B. Torrance, Physica C **160**, 30 (1989).
[15]K. Suzuki, K. Kishio, T. Hasegawa, and K. Kitazawa, Physica C **166**, 357 (1990).
[16]E. Wang, J. M. Tarascon, L. H. Greene, and G. W. Hul, Phys. Rev. B **41**, 6582 (1990).
[17]N. A. Fortune, K. Murata, M. Ishibashi, Y. Yokoyama, and N. Nishihara (unpublished).
[18]H. Oyanagi, K. Oka, H. Unoki, Y. Nishihara, K. Murata, M. Tokumoto, and Y. Kimura, J. Phys. Soc. Jpn. **58**, 2896 (1989).
[19]N. Kosugi, H. Kondo, H. Tajima, and H. Kuroda, Chem. Phys. **135**, 149 (1989).
[20]H. Oyanagi, H. Ihara, T. Matsubara, M. Tokumoto, T. Matsushita, M. Hirabayashi, K. Murata, N. Terada, T. Yao, H. Iwasaki, and Y. Kimura, Jpn. J. Appl. Phys. **26**, L1561 (1987).
[21]Y. Yokoyama *et al.* (unpublished).
[22]J. D. Jorgensen, B. Dabrowski, S. Pei, D. R. Richards, and D. G. Hinks, Phys. Rev. B **40**, 2187 (1989).
[23]J. Kondo and S. Nagai, J. Phys. Soc. Jpn. **57**, 4334 (1988).
[24]Z. Tan, M. E. Filipkowski, J. I. Budnick, E. K. Heller, D. L. Brewe, B. L. Chamberland, C. E. Bouldin, J. C. Woicik, and D. Shi, Phys. Rev. Lett. **64**, 2715 (1990).